EG UK Computer Graphics & Visual Computing (2015)
Rita Borgo, Cagatay Turkay (Editors)

Tiled Projection Onto Deforming Screens

H. Kim[1] and C. Schinko[1] and S. Havemann[1] and I. Redi[2] and A. Redi[2] and D. W. Fellner[1,3]

[1]Institute of ComputerGraphics and KnowledgeVisualization (CGV), TU Graz, Austria
[2]ORTLOS Architects and Space Engineering, Graz, Austria
[3]TU Darmstadt & Fraunhofer IGD, Germany

Abstract

For the next generation of visual installations it will not be sufficient to surround the visitor by stunning responsive audiovisual experiences – the next step is that space itself deforms in response to the user or user groups. Dynamic reconfigurable spaces are a new exciting possibility to influence the behaviour of groups and individuals; they may have the potential of stimulating various different social interactions and behaviours in a user-adapted fashion. However, some technical hurdles must be overcome.

Projecting on larger surfaces, like a ceiling screen of 6 × 8 *meters, is typically possible only with a tiled projection, i.e., with multiple projectors creating one large seamless image. This works well with a static ceiling; however, when the ceiling dynamically moves and deforms, the tiling becomes visible since the images no longer match. In this paper we present a method that can avoid such artifacts by dynamically adjusting the tiled projection to the deforming surface. Our method is surprisingly simple and efficient, and it does not require any image processing at runtime, nor any 3D reconstruction of the surface at any point.*

Categories and Subject Descriptors (according to ACM CCS): I.3.3 [Computer Graphics]: Picture/Image Generation—Display algorithms

1. Introduction

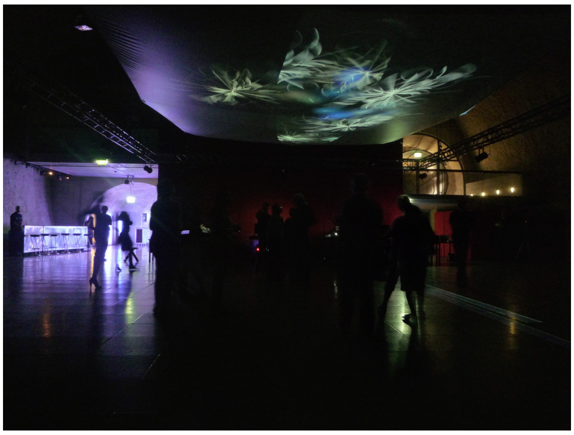

Figure 1: *The Responsive Open Space installation with seamless short-throw, high-res rear projection on a bent 8×6 m ceiling screen. The projection surface deforms interactively in response to the engagement of participants.*

Tiled displays can be used for more than large images; they can in fact become part of architecture. Combining multi-projection with other technologies, such as touch interaction and holographic stereograms, can provide augmented information by visualizing responsive imagery. Yet another dimension are deformable displays, which allow the projection surface to be geometrically deformed. This practically expands the viewing experience from 2D to 3D. The display becomes an integral part of a novel media architecture that responds dynamically to user interaction.

The registration of dynamic displays has triggered much research and development. Nevertheless, several challenges remain. First, most of the existing work uses well-calibrated projectors and sensors in a permanently installed environment. Often, however, a large tiled projection system is needed only temporarily for short term events like stage performances and exhibitions. An exhibition at a rented place potentially costs a lot of money, thus the setup time is very limited and it imposes special demands on hardware as well as human resources. Reducing the required hardware and calibration is desirable for quick installation and removal. Second, in a rented exhibition location it is very common

DOI: 10.2312/cgvc.20151239

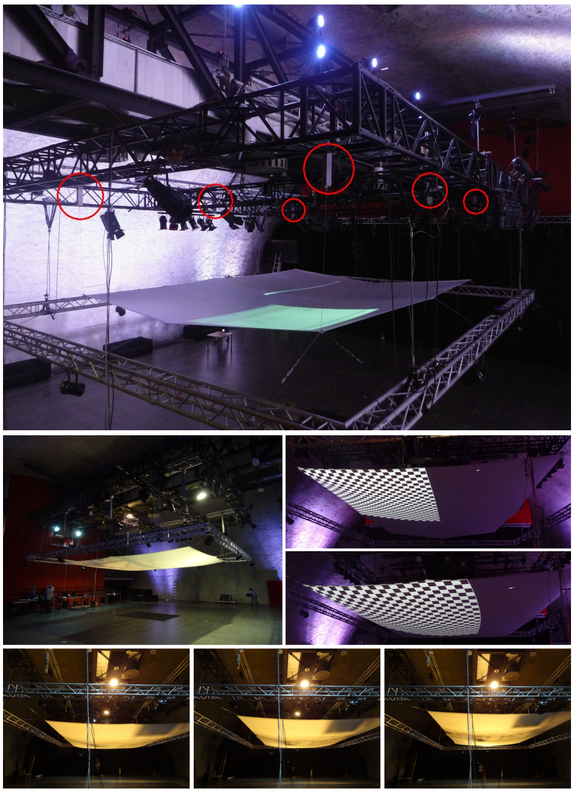

Figure 2: *The projection setup of the event consists of four projectors projecting onto a movable fabric used as projection surface. It is suspended between electronically controlled actuators (marked by red circles) that can move vertically. A single high-resolution camera with a very wide angle lens is mounted between the four projectors, observing the whole projection surface to obtain the necessary information for geometric registration and brightness compensation.*

that much of the equipment, such as stage lighting or the sound system, is stationary and hardly movable. Not only the hardware, but also the software needs to be robust and adjustable to the various configuration requirements.

The framework presented in this paper has been developed in the context of a project called *Responsive Open Space* initiated by ORTLOS Space Engineering Graz/London. A large projection surface (8×6 m) was suspended between telescope rods at the location *Dom im Berg* in Graz (see Figure 1), and used for an interactive visualization triggered by human social interaction, captured by a Kinect sensor. Four projectors were used for a rear-projection onto a ceiling display. It showed visuals from a team of creative artists who participated in the project. The suspended projection surface was heavily deformed and non-planar due to its size and weight, which was quite appealing but also presented a major technical challenge.

The system proposed in this paper can cope this challenge and maintain a perfect 2×2 tiling also when the screen deforms. Our contribution is a simple and robust method that is split into an offline and an online phase. Our method is 2D and does not require a 3D reconstruction of the environment. It is based on the observation that although the screen deforms in a very non-linear way, we can still compensate for the image distortion by multi-linear interpolation. In our case it is hexalinear because of the six telescope rods used (see Figure 2). We assume that the same holds true for other deformable display setups with fewer or more degrees of freedom d. The interpolation scheme can easily be adapted to this, but a sufficient number of measurements must be taken (typically 2^d).

2. Related Work

Large-scale tiled displays on non-planar screens have become feasible through the use of high-resolution cameras for calibration. They capture structured patterns projected onto the unknown projection surface. The calibration allows for geometric alignment of the projectors. In order to deal with moving and deforming display surfaces, the pattern acquisition must allow for realtime operation. Ideally, the geometric correction requires capturing only a single image. Since the calibration of dynamically deforming surfaces resembles to 3D scanning, there are some techniques that are adoptable in both cases. They range from traditional techniques for stereoscopic devices [SS03, GVG06] to point cloud reconstruction [QJS*06]. For tiled projection displays, the projector is used both for the geometric correction and for the display of content. To accomplish both display and measurement simultaneously, imperceptible structured light techniques were developed. Raskar et al. presented a combination of time-division multiplexing and light cancellation techniques to hide the patterns in a rapid series of white-light projections with a synchronized camera [RWC*98]. This method can be scaled to build seamless panoramic display system by using multiple cameras and projectors [RBY*99]. However, for realtime update of changes in display geometry, the pattern needs to be projected in such a high frequency that it noticeably disturbs the content projection. Using the physical calibration pattern to define a common world coordinate system, to which all display tiles are registered, is also not applicable to our rear-projection ceiling display environment. Cotting et al. proposed a method to imperceptibly embed arbitrary binary patterns into ordinary color images displayed by unmodified off-the-shelf Digital Light Processing (DLP) projectors. The encoded images are visible only to cameras synchronized with the projectors, while the original images appear only minimally degraded to the human eye [CNGF04, CFZG05]. However, this is not applicable in our case since we use multiple projectors whose display boards are not synchronized. In Lee's method, a small set of optical sensors are embedded in the display screen and a series of gray-coded binary patterns are projected to discover the projection area [LDMA*04]. This technique can be scaled to multiple projectors with arbitrary display geometry, but it works only for front-projection since the sensors are embedded in the screen. Garcia-Dorado et al. used fiducial markers tracked by the camera to define the boundaries of the display region [GDC11]. Their method seems to potentially support arbitrary shaped projected regions, but has a constraint that the fiducial markers should be placed within the display area of the projectors. This seems not suitable for our overlapping 2×2 configuration. The continuous display surface autocalibration method does not require dedicated hardware such as IR light sources and filters or synchronized cameras. It simply uses a camera that observes the display and matches image features with the corresponding features that appear on the display [YG01]. But this method needs an image stream with distinguishable geometric features corresponding between consecutive frames, in order to continuously refine an estimate of the display surface geometry. Zhou also proposed a continuous self-calibration method with a camera rigidly attached to a projector; but it works only for planar surfaces and needs re-scanning when the surface geometry is changed [ZWAY08], thus disturbing the content display. Using a camera attached to the projector is particularly useful if the projector or the display screen moves, since the camera can obtain the information of the projection space right at the point of view of the projector. For example, Raskar et al. created a self-correcting projector by mounting a camera with tilt sensors, so that pre-warped images can be projected onto planar surfaces of arbitrary inclination [RB01]. However, since the pre-warping required for the correct projection is defined by the homography between the projector image and camera image, the method is limited to planar surfaces [SSM01].

3. Reconfigurable Projection Geometry

An overview of the processing pipeline is shown in Figure 3. First of all, the camera is calibrated by measuring its intrinsic parameters. Then the offline phase proceeds by projecting a sequence of patterns on the display surface with the actuators in certain lift configurations. For each configuration, pattern recognition is performed to extract the grid positions of the feature points in the image captured for each projector. This produces a checkerboard grid that describes the geometric shape distortion from the respective lift configuration. Surprisingly, these grids also allow for undistorting the projected images without any further computations, since they can be directly used as (u,v) texture coordinates (see Section 3.3).

During runtime, the tiled images of the multi-projector display must appear seamless, as if they were projected from a single projector. The main key for achieving such well-stitched imagery is to determine the geometric relationship between the overlapping projectors as accurately as possible. The online adaptation procedure requires three steps:

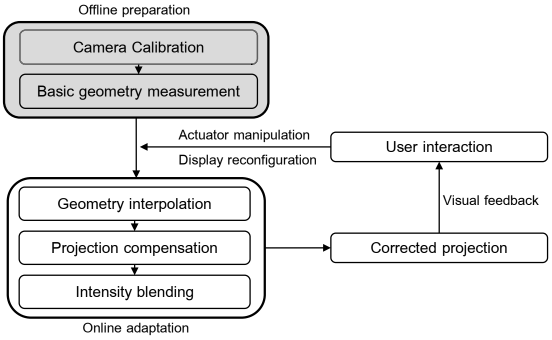

Figure 3: *Process overview.*

- Estimating the surface deformation
- Compensating the deformations
- Blending the image intensities (soft edge blending)

These steps are described in detail in the following. – Note that most software created in the context of the project is open source and can be downloaded from our website [†].

3.1. Measuring Surface Geometry for Low-Frequency Bending

The geometry of the display surface can be estimated by identifying the positions of projected feature points in the captured camera image. The grid simplifies the geometric registration considering the surface as an arrangement of piecewise planar surfaces. The checkerboard pattern facilitates this further since the feature points are located at the corners of quadratic patches. More geometric detail of the display surface can be capture simply by using a higher grid resolution. The resolution is a trade-off between complexity of the display surface, projector resolution and camera resolution. The checkerboard should be made up of equal-sided quadrangles, i.e., squares, so the width and height of the projector image should be divided by one of their common divisors, which then becomes the size of the squares. Our projectors have the resolution 1280×720, and we use a checkerboard resolution of 32x18 squares with 40×40 pixels each. Our corner recognition method is described in our previous work [KSHF13].

3.2. Online Adaptation

The detailed inspection of measured grid data lead to an important observation illustrated in Figure 4. We examined the effect of varying a single rod parameter on the grid points of a given configuration. The shape of the flexible surface is

[†] http://www.cgv.tugraz.at/CGV/Research/Projects/Responsive Open Space

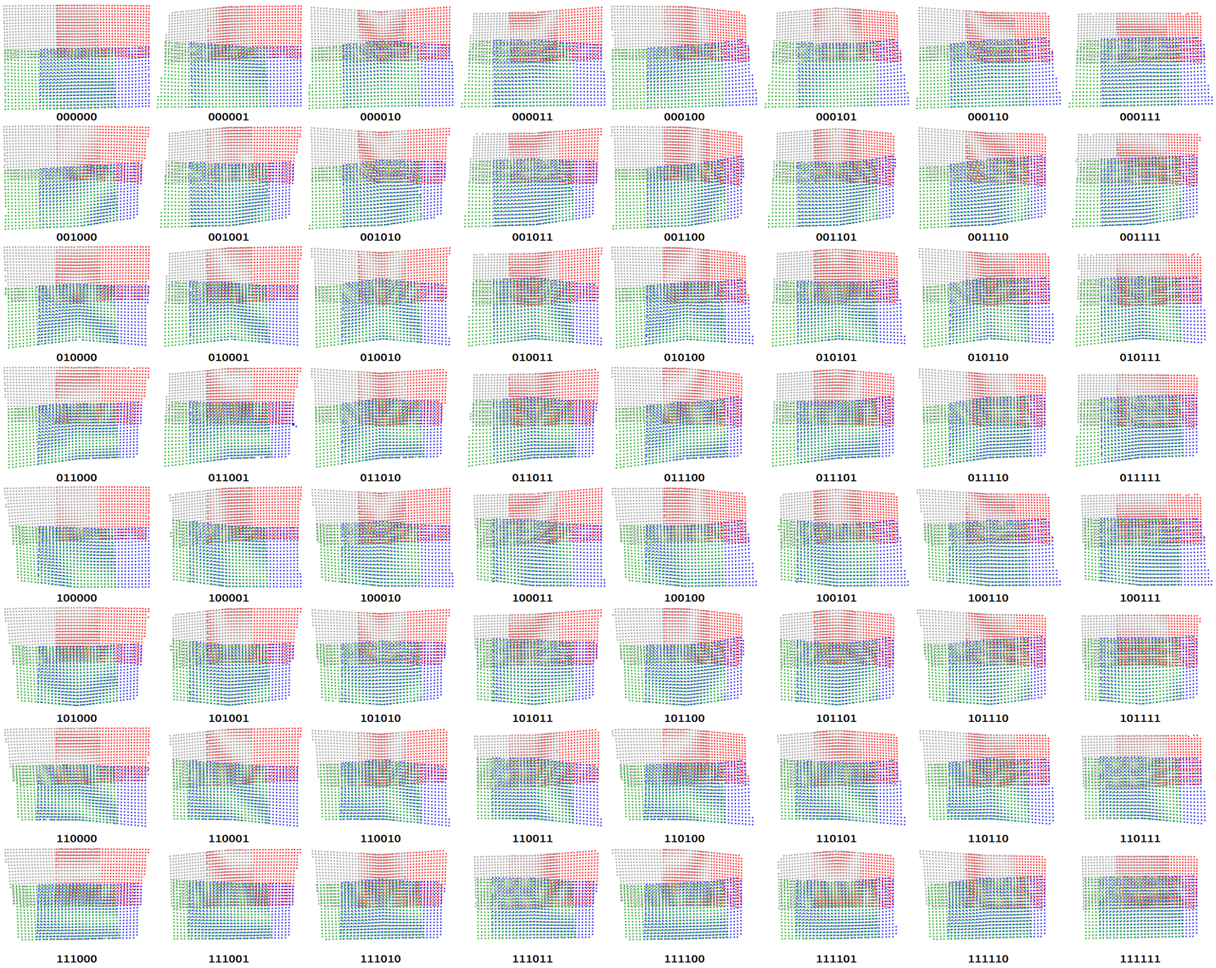

Figure 6: *The 64 grid measurements for all combinations of the six rods in extreme positions, namely* 0.0 *(closest) and* 1.0 *(farthest away).*

determined by six parameters noted as a 6-tuple of floating-point numbers, e.g. $(1,0,1,0,1,0) \in [0,1]^6$. When one parameter is varied, e.g. $(1,0,1,t,1,0)$ for $t \in [0,1]$, it turns out that the grid points travel *linearly* between the two grids for $t = 0$ and $t = 1$. Figure 4 (bottom) shows that the points for $t = 0.5$ not only lie on, but are even in the middle of the respective line segments. So although the surface is bent, i.e., its shape is not linear, and it also moves in a nonlinear way, the grid points move along a straight line. This is because the points 'inherit' their linearity from the straight light rays of the projector. Figure 5 illustrates the obvious fact that the intersections of the bent moving surface with the light rays sent out by projector P all lie on a straight line; and when seen from the camera C, this linearity is preserved. Although each of the six parameters pulls the grids in different directions, all grid points individually move linearly with respect to the variation of any single parameter. A specific configuration $(t_1,t_2,t_3,t_4,t_5,t_6)$ can be obtained by six successive changes:

$$(0,0,0,0,0,0) \rightarrow (t_1,0,0,0,0,0) \rightarrow \ldots \rightarrow (t_1,t_2,t_3,t_4,t_5,t_6)$$

Since each change is linear, and they can be carried out in any order (as the surface shape is deterministic), they must be the result of multi-linear, in this case hexalinear, interpolation.

To recapitulate, tri-linear interpolation yields a function value for $(t_1,t_2,t_3) \in [0,1]^3$ by interpolating between the function values at the $2^3 = 8$ corners of the 3-dimensional unit cube (the order of the coordinates does not matter):

$$\begin{aligned}
f(t_1,0,0) &= (1-t_1)f(0,0,0)+t_1 f(1,0,0)\\
f(t_1,0,1) &= (1-t_1)f(0,0,1)+t_1 f(1,0,1)\\
f(t_1,1,0) &= (1-t_1)f(0,1,0)+t_1 f(1,1,0)\\
f(t_1,1,1) &= (1-t_1)f(0,1,1)+t_1 f(1,1,1)\\
f(t_1,t_2,0) &= (1-t_2)f(t_1,0,0)+t_2 f(t_1,1,0)\\
f(t_1,t_2,1) &= (1-t_2)f(t_1,0,1)+t_2 f(t_1,1,1)\\
f(t_1,t_2,t_3) &= (1-t_3)f(t_1,t_2,0)+t_3 f(t_1,t_2,1)
\end{aligned}$$

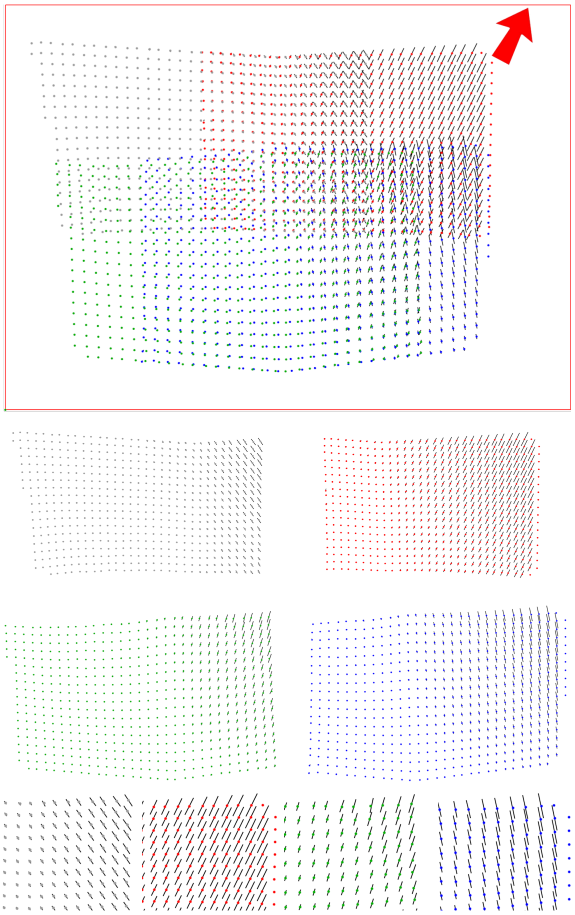

Figure 4: *Linear grid variance observation. The configuration* $(1,0,1,t,1,0)$ *is shown. Reducing t moves a corner of the surface closer, which pulls the grid points towards the top right (arrow). The grid for* $t = 0.5$ *(dots) is compared to the grids for* $t = 0$ *and* $t = 1$*, which are connected by short black line segments. Middle: The points move in the direction of the lens (optical center) of the respective projector. Bottom: The grid close-ups (top right corner) reveal that the points travel* linearly *on their segments.*

Similarly, the 6D unit cube has $2^6 = 64$ corners corresponding to all possible combinations of six zeros and ones. To obtain the function value for a given parameter tuple $(t_1,t_2,t_3,t_4,t_5,t_6) \in [0,1]^6$, linear interpolation along the first coordinate yields 32 interpolants, then 16 along the 2nd, 8 along the 3rd, 4 along the 4th, 2 along the 5th, and finally one along the direction of the last coordinate; 63 linear interpolations are needed in total. Since we are interpolating between grids, this has to be carried out for u and for v, which amounts to $4 \cdot 63 = 252$ multiplications and $2 \cdot 63 = 126$ additions to obtain a grid point. Performing this for all points effectively yields a grid that is the hexalinear blend between all 64 grids shown in Figure 6. As it is parallelizable, this can nevertheless be easily accomplished in real time.

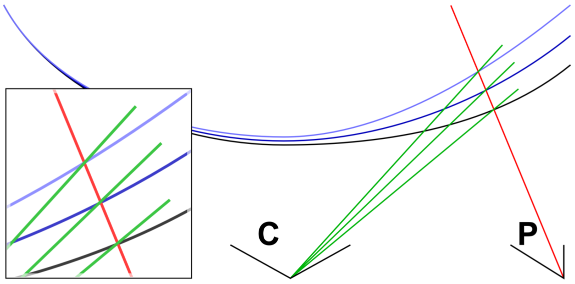

Figure 5: *Explanation of the observed linearity. The ray from projector P (red) intersects the deforming surface on a straight line; locally, the displacement is linear with respect to the displacement of the rod, which explains the linearity observed by the camera C (green).*

3.3. Projection Compensation

The visual artists developed their visualizations using their favorite platform, the *Processing* [RFM07] toolkit. The visualizations were developed as so-called "sketches" on a single-display laptop, and the goal was to port them without any development overhead to the tiled deformable projection system.

A Processing script operates on a rectangular client viewport. We map it to the four projectors using the measured pixel coordinates of the four interpolated grids. For each projector, the respective grid points are handed over to the script as texture coordinates for displaying a part of the viewport. The client viewport is defined in camera pixel coordinates. A framebuffer in the size of the camera image is used for off-screen rendering of the Processing sketch. We use hooks inside our script to call the visual sketch to render it into the framebuffer. Our display routine then uses this framebuffer as a texture for a pre-defined planar quad mesh whose vertex positions are just the previously calculated texture coordinates. This directly compensates the deformation of the projection surface from the viewpoint of the camera, as illustrated in Figure 7.

Once the deformed projection is visually compensated, the pixel intensities in the overlap regions have to be attenuated using alpha blending to obtain a consistent brightness over the whole surface. The detail process for intensity blending is described in our previous work [KSHF13].

3.4. User Interaction

User interaction takes place after a corrected projection setup is established. Our test setup allows user feedback in the form of manual displacement of the screen. In the Responsive Open Space setup, user input is incorporated using a Microsoft Kinect sensor capturing the movement of users below the projection surface. This data is analyzed by a 3rd party software to determine the 'social interaction status' of

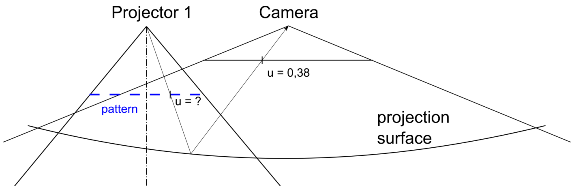

Figure 7: *The projection compensation is depicted for one dimension only. A pattern is projected onto the screen and a picture is taken with the camera. For each grid point of the pattern, its u-coordinate is measured in the camera image. These coordinates can be directly used as texture coordinates in the Processing script of the respective grid point, thus generating an undistorted projection from the viewpoint of the camera.*

the crowd. This provides the input data to control the position of the actuators, e.g., to lower the screen above a detected group of persons. The positions of the actuators serve as input for the online adaptation to compensate the dynamic changes of the projection environment.

4. Results

We have built a smaller test setup to improve the accuracy and to optimize the performance of our system. Figure 11 shows the scaled down version of the Responsive Open Space setup with a suspended screen of 1.2×0.90 meters. Basically the same 2×2 projector configuration was realized, but as a front-projection, i.e., projecting (and looking) from below. For capturing the images we used a 10 megapixel industrial camera (3840×2748) with a wide angle lens, whose intrinsic parameters were calibrated in advance.

In order to obtain enough reliable ground truth data for validating the online projection adaption, and to evaluate the accuracy of the estimation, we have measured $3^6 = 729$ configurations resulting from all combinations of the values $t_{1...6} \in \{0, 0.5, 1\}$. With one image per projector this yields 2916 images in total, which were processed to extract the checkerboard grid. This took about 40 seconds per image, leading to a total of less than 3 minutes per configuration. Only the $2^6 \cdot 4 = 256$ grids shown in Fig. 6 were used for the online grid adaptation by interpolation; the other grids were used just for validation. Table 1 shows the mean error of the 2D distance between the interpolated and the measured grid points. The six numbers in the second column are the rod parameters, i.e., the heights of the six hooks between which the screen is suspended. These six parameters determine the shape of the surface in a quite repeatable way, as we found, although the test setup required manual setting of the parameters. This manual manipulation has possibly affected the repeatability of the screen adjustment, which led to the slight numerical error. Unpredictable effects of the used fabric, such as fine wrinkles, slack and stretch, could also have an influence on the result. Nevertheless, according to Table 1 the mean error is only about $3-4$ pixels, i.e., 0.1% of the camera image resolution. This is hardly noticeable to the human eye, as shown in Figure 8. Consequently, our test setup has reached the main goal of any tiled projection, a seamless image across all tiles.

To determine the boundaries and limitations of our method we have tested it with an extreme vertical displacement. At a maximum displacement of 70 percent of the width of the sheet (0.63 meters) for each rod, the horizontal angle of the screen is almost 45 degrees. This has several adverse consequences such as too much slack, thick wrinkles, and partial overlaps on large parts of the screen. The checkerboard pattern does not have sufficient resolution for the geometric complexity caused by the wrinkles and overlaps. This leads to the errors of the grid structure shown in Figure 9. We discovered that the linear interpolation between two configurations in such a large distance is not working properly anymore. Figure 10 (left) shows the resulting projection image for configuration (0,0,0.5,0.5,0,0) using the measured values. The hexalinear interpolation fails to properly estimate the measured values from the 64 measured extreme configurations, as shown in Figure 10 (right). We expect that restoring linearity can be achieved by taking more measurements, e.g., at values $t_i \in [0, 0.5, 1]$ instead of only at $t_i \in [0, 1]$. However, this increases the measurement effort dramatically ($3^6 = 729$ instead of $2^6 = 64$ configurations).

5. Conclusion

We have presented a new method for the tiled projection on screens with variable geometry. Our method uses a piecewise linear approximation to pre-calculate the response to shape changes of the projection surface. Although the surface is highly nonplanar and deforms non-linearly, the intersection of the moving surface with a straight ray varies linearly with the displacement of each of the rods, which is exploited in a hexalinear interpolation. We consider our method to be useful for a range of similar setups following the same basic principle. To extend the method, we consider

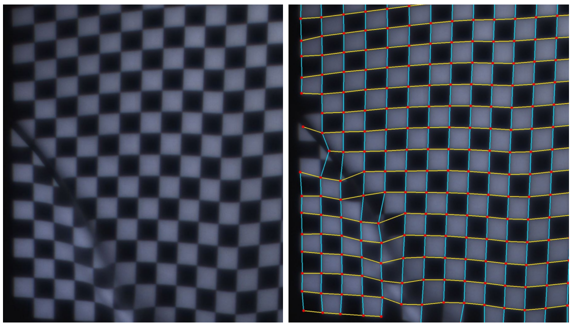

Figure 9: *Heavily deformed surface (left) resulting in reconstructed checkerboard pattern with errors (right).*

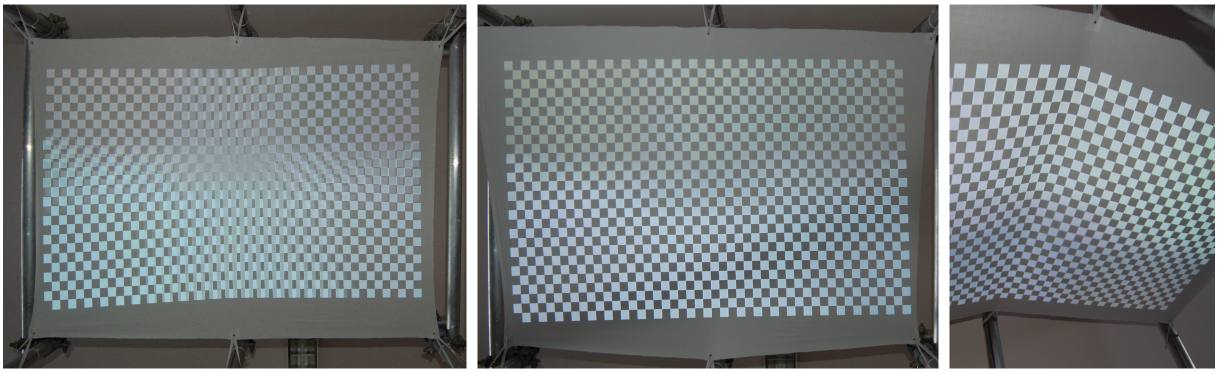

Figure 8: *Geometric correction of overlapping images. Severe artefacts (left) disappear with the hexalinear interpolation of 64 measured grids (middle, right).*

No	Configuration						Mean Error				Maximum Error			
	$(t_1$	t_2	t_3	t_4	t_5	$t_6)$	P_1	P_2	P_3	P_4	P_1	P_2	P_3	P_4
1	1	0	0	0	0	0	0.0	0.0	0.0	0.0	0.0	0.0	0.0	0.0
2	0	1	0	0	1	0	0.0	0.0	0.0	0.0	0.0	0.0	0.0	0.0
3	0.25	0.25	0.25	0.25	0.25	0.25	6.7	5.8	3.9	3.4	26.0	19.0	17.1	17.0
4	0.5	0.5	0.5	0.5	0.5	0.5	1.8	1.7	2.2	1.8	7.2	12.1	8.9	10.0
5	0.75	0.75	0.75	0.75	0.75	0.75	2.7	3.8	2.7	3.8	18.4	9.9	9.9	7.6
6	1	0.5	1	0	0.5	0.5	3.2	4.6	2.9	2.2	7.6	15.7	8.1	9.9
7	1	0	1	0.5	0	0.5	1.5	2.3	2.0	2.3	8.5	11.4	14.0	8.2
8	0	0.5	1	1	0.5	0	4.2	2.9	2.3	2.0	13.0	11.2	15.1	10.0
9	1	0.5	0	0	0.5	1	2.5	2.0	3.6	2.7	8.6	12.5	10.0	8.9
10	0	1	0.5	1	0	0.5	1.8	2.1	2.1	1.6	10.0	10.0	15.3	7.6
11	0.5	0	0.5	0	0.5	0	5.8	5.2	5.8	3.9	16.5	13.0	14.6	13.0
12	0.5	0	1	0.5	0	1	1.7	1.8	1.9	1.6	17.3	12.0	8.1	9.2
13	0.2	0.3	0.8	1	0	0.6	3.8	4.7	3.3	2.4	17.5	13.6	13.0	6.1
14	0.6	0.5	1	0.3	0.25	0.75	3.7	4.7	3.6	4.3	9.8	19.4	9.9	12.1
15	0.3	1	0	0.5	0.8	0	2.9	3.7	5.6	2.4	13.0	18.1	8.3	7.6
16	0	0	1	0	0.5	0.5	4.8	5.7	4.3	3.0	15.8	14.4	10.8	10.2
17	0.5	0.5	0	0	0	0	3.2	5.9	4.5	5.4	10.4	18.8	15.0	13.3
18	0	0	0.75	0	0	0	4.4	5.3	3.8	3.0	15.8	23.3	10.0	18.0
19	0.5	0	0	0	0	0	3.8	4.0	5.0	2.9	9.4	17.7	20.4	13.4
20	0	0.5	0	0	0	0	4.6	4.7	4.1	4.0	18.0	19.4	15.5	13.4
21	0	0	0.5	0	0	0	3.5	2.6	3.1	4.0	15.0	17.0	11.4	12.5
22	0	0	0	0.5	0	0	2.3	2.4	2.3	1.8	12.2	8.9	15.6	8.1
23	0	0	0	0	0.5	0	3.3	3.7	3.5	3.5	16.3	17.7	12.4	12.5
24	0	0	0	0	0	0.5	3.9	2.9	3.4	3.7	18.4	13.4	18.7	10.0

Table 1: *Mean and maximum distance between the measured geometries and the estimated results (in camera pixels). The display surface is continuously deformable between the lowest status* $(0,0,0,0,0,0)$ *and the highest status* $(1,1,1,1,1,1)$. *The known surface geometries have zero error [1-2]. The degree of deformation, i.e., the number of intermediate (interpolated) values, has almost no effect on the estimation accuracy [3-18]. If any input value changes, then the projection on all four screens must be updated [9-24].*

projecting onto larger collections of pieces of more stretchable fabric that are connected in a tent-like manner; this can be used to realize whole illuminated "domes" of fabric, which can convey a very powerful spatial impression. Another important question is how to measure the rod displacements when they are not known - either because the rods have no feedback channel, or because we are in a more complex environment. We envisage, e.g., developing "good-looking" markers that can be projected without interfering noticeably with the artistic visual content.

In the future, we will also build an interactive bent projection screen using multiple cheap LED projectors in an overlapping but not tiled configuration. The screen shall move in response to human interaction captured by a range sensor (RGB+D camera). Methods for extracting the surface ge-

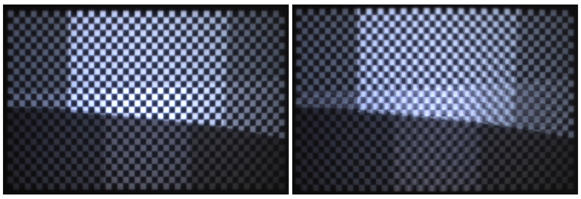

Figure 10: *In a more extremely displaced test scenario (maximum vertical distance 0.63 meters), even the projection image using measured (u,v) values (left) shows artefacts from misregistration (grid errors), and the interpolation (right) fails completeley.*

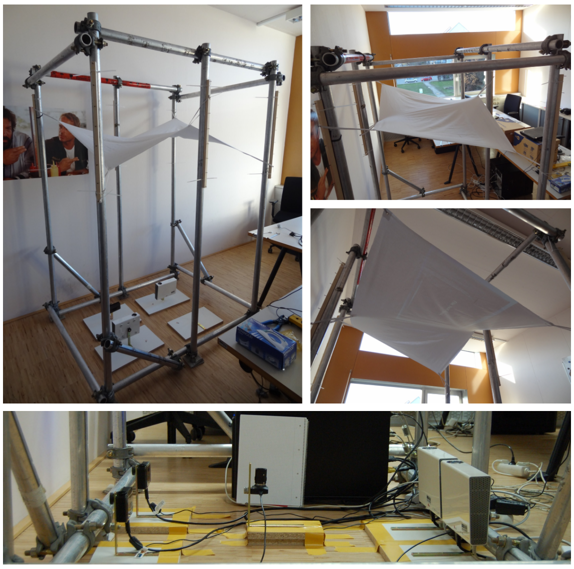

Figure 11: *The demo setup for controlled measurement. The sheet is not very stretchable; it is suspended with rubber tapes that can be adjusted manually. The vertical displacement of the scale model corresponds to 2 meters of the real setup (Figures 1 and 2); the sheet deforms significantly. Bottom: The final configuration of the four projectors with the wide-angle camera in the center.*

ometry and adapting for the quad mesh texture in realtime should be studied as well. Dynamically deformable screens are an exciting new artistic 'architectural medium' that can greatly enhance the impression of interactive visuals. So we think there is a good chance that movable walls may indeed become common. We hope we have helped to prepare the ground for that.

References

[CFZG05] Cotting D., Fuchs H., Ziegler R., Gross M. H.: Adaptive instant displays: Continuously calibrated projections using per-pixel light control. *Computer Graphics Forum 24*, 3 (2005), 705–714. 2

[CNGF04] Cotting D., Naef M., Gross M., Fuchs H.: Embedding imperceptible patterns into projected images for simultaneous acquisition and display. In *Proceedings of the 3rd IEEE/ACM International Symposium on Mixed and Augmented Reality* (Washington, DC, USA, 2004), ISMAR '04, IEEE Computer Society, pp. 100–109. 2

[GDC11] Garcia-Dorado I., Cooperstock J.: Fully automatic multi-projector calibration with an uncalibrated camera. In *Computer Vision and Pattern Recognition* (2011), pp. 29–36. 3

[GVG06] Griesser A., Van Gool L.: Automatic interactive calibration of multi-projector-camera systems. In *Proceedings of the 2006 Conference on Computer Vision and Pattern Recognition Workshop* (Washington, DC, USA, 2006), CVPRW '06, IEEE Computer Society, pp. 8–. 2

[KSHF13] Kim H., Schinko C., Havemann S., Fellner D. W.: Tiled projection onto bent screens using multi-projectors. In *IADIS International Conferences Computer Graphics, Visualization, Computer Vision and Image Processing* (2013), pp. 67 – 74. 3, 5

[LDMA*04] Lee J. C., Dietz P. H., Maynes-Aminzade D., Raskar R., Hudson S. E.: Automatic projector calibration with embedded light sensors. In *Proceedings of the 17th annual ACM symposium on User interface software and technology* (2004), UIST '04, pp. 123–126. 3

[QJS*06] Quirk P., Johnson T., Skarbez R., Towles H., Gyarfas F., Fuchs H.: Ransac-assisted display model reconstruction for projective display. In *Proceedings of the IEEE conference on Virtual Reality* (Washington, DC, USA, 2006), VR '06, IEEE Computer Society, pp. 318–. 2

[RB01] Raskar R., Beardsley P.: A self-correcting projector. *IEEE Conference on Computer Vision and Pattern Recognition 2* (2001), 504–508. 3

[RBY*99] Raskar R., Brown M., Yang R., Chen W.-C., Welch G., Towles H., Scales B., Fuchs H.: Multi-projector displays using camera-based registration. In *Visualization '99. Proceedings* (1999), pp. 161–522. 2

[RFM07] Reas C., Fry B., Maeda J.: *Processing: A Programming Handbook for Visual Designers and Artists*. The MIT Press, 2007. 5

[RWC*98] Raskar R., Welch G., Cutts M., Lake A., Stesin L., Fuchs H.: The office of the future: a unified approach to image-based modeling and spatially immersive displays. In *Proceedings of the 25th annual conference on Computer graphics and interactive techniques* (New York, NY, USA, 1998), SIGGRAPH '98, ACM, pp. 179–188. 2

[SS03] Scharstein D., Szeliski R.: High-accuracy stereo depth maps using structured light. In *Proceedings of the 2003 IEEE computer society conference on Computer vision and pattern recognition* (Washington, DC, USA, 2003), CVPR'03, IEEE Computer Society, pp. 195–202. 2

[SSM01] Sukthankar R., Stockton R. G., Mullin M. D.: Smarter presentations: Exploiting homography in camera-projector systems. In *ICCV* (2001), pp. 247–253. 3

[YG01] Yang R., GregWelch: Automatic and continuous projector display surface calibration using every-day imagery. In *Proceedings of the 9th International Conference in Central Europe on Computer Graphics, Visualization and Computer Vision* (2001). 3

[ZWAY08] Zhou J., Wang L., Akbarzadeh A., Yang R.: Multi-projector display with continuous self-calibration. In *Proceedings of the 5th ACM/IEEE International Workshop on Projector camera systems* (New York, NY, USA, 2008), PROCAMS '08, ACM, pp. 31–37. 3